Eur. Phys. J. B (2015) 88: 318
DOI: 10.1140/epjb/e2015-60560-0

THE EUROPEAN PHYSICAL JOURNAL B

Regular Article

Quantum theory of spin alignment in a circular magnetic nanotube

Gerd Bergmann[a], Richard S. Thompson[b], and Jia G. Lu

Department of Physics and Astronomy, University of Southern California, 90089-0484 Los Angeles, California, USA

Received 11 July 2015 / Received in final form 22 September 2015
Published online 2 December 2015 –

Abstract. When electron spin and momentum couple in a solid, one generally obtains intriguing and unexpected phenomena. Metallic ferromagnetic nanotubes of cobalt with circular magnetization, which have been prepared by us and others, are a particularly interesting system. Here the spins of the conduction electrons are frustrated. They would like to align parallel to the magnetic field of the magnetization, but as the electrons move quickly around the tube the spins cannot follow the magnetization direction. In a previous short theoretical paper we solved the spin dynamics using a classical model. Here we generalize our work to a quantum mechanical model. The surprising result is that the spin of most conduction electrons is not parallel or anti-parallel to the circumferential magnetization but mostly parallel or anti-parallel to the axis of the nanotube. This result means that such a cobalt nanotube is a different ferromagnet from a cobalt film or bulk cobalt.

1 Introduction

Magnetic nanostructures show exciting physical properties and have many potential applications in engineering such as magnetization switching, memory devices and spintronic elements [1–7]. Furthermore there are applications in medicine such as magnetic-based gene delivery, new diagnostic tools, magnetic-field assisted bioseparation, biointeraction, and drug delivery [8–11], and in neuroscience magnetic stimulation of ganglion neurons [12].

The orientation of the magnetization is particularly interesting in ferromagnetic nanotubes. A number of experimental studies have shown that states exist in these materials where the magnetic polarization is oriented circumferentially around the axis of the tube [6,13–17]. In these materials one has together with the circular magnetization an exchange field $\mathbf{B} = B_0\widehat{\phi}$ that is parallel to the surface along the circumference. The interplay between the spin of the conduction electrons and the magnetization of these nanotubes represents a fascinating problem.

The magnetic moment $\vec{\mu}$ and spin of the electron have opposite directions $\vec{\mu} = \gamma\mathbf{s}$ (with the gyromagnetic ratio $\gamma = -2\mu_B/\hbar = -e/m$). It is often more convenient to use the spin $\mathbf{s}$ in physical drawings such as Figure 1 and in discussions. The spin feels a torque in the presence of the magnetic field $\mathbf{B}$ due to the magnetization and reacts with a change of direction as

$$\frac{d\mathbf{s}}{dt} = \vec{\mu}\times\mathbf{B} = \mathbf{s}\times\left(\gamma B_0\widehat{\phi}\right) = \mathbf{s}\times\vec{\omega}_B$$

where we introduce the spin field

$$\vec{\omega}_B = \gamma B_0\widehat{\phi} = -\left(2\mu_B B_0/\hbar\right)\widehat{\phi} \tag{1}$$

which is opposite to the magnetic field.

In a previous investigation [18] we studied the dynamics of the conduction electron spin in a classical calculation. We found interesting and unusual results. The electron propagates with angular velocity $\vec{\omega}_e = (v_\phi/R)\widehat{\phi}$ around the nanotube (v_ϕ is the electron velocity along the circumference of the cylinder). On first thought, one might expect the electron spin $\mathbf{s}$ to align with the direction of the circular spin field $\vec{\omega}_B = \gamma B_0\widehat{\phi}$ (opposite to magnetization) while traveling around the nanotube. However, it turned out that the spin dynamics do not allow this behavior because the electron with the velocity v_ϕ travels too fast for the spin to follow the changing direction of $\vec{\omega}_B$.

We found it convenient to study the spin dynamics in a coordinate system that is travelling along with the electron and also spinning to follow the magnetization direction. Then the axes of an electron's coordinate system $(\widehat{\mathbf{x}},\widehat{\mathbf{y}},\widehat{\mathbf{z}})$ are parallel to the unit vectors in cylindrical coordinates $(\widehat{\mathbf{r}},\widehat{\phi},\widehat{\mathbf{z}})$. This system moves with the electron and spins with $\vec{\omega}_e = \omega_e\widehat{\mathbf{z}}$. We call the orbiting and spinning frame S in contrast to the inertial laboratory frame S_0. The resulting behavior of the electron spin is shown in Figure 1.

In the spinning non-inertial frame S the electron spin experiences an inertial torque of $-\vec{\omega}_e\times\mathbf{s}$, which can be expressed as a large spin field $\omega_e\widehat{\mathbf{z}}$ in the z-direction. Together the inertial spin field $\omega_e\widehat{\mathbf{z}}$ and the

[a] e-mail: bergmann@usc.edu
[b] e-mail: rsthom@usc.edu

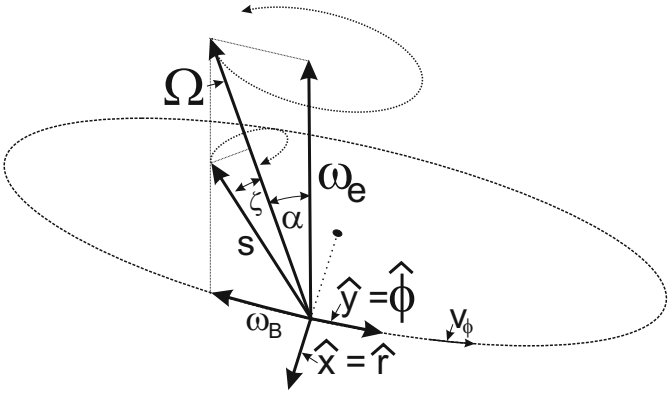

Fig. 1. The dynamics of the electron spin in the classical calculation. The circular magnetic field acts on the spin as a spin field $\vec{\omega}_B$ and the spinning frame introduces an inertial spin field $\vec{\omega}_e$. Both are shown in the figure and add up to $\mathbf{\Omega}$. In the orbiting and spinning frame S all spin fields are constant. In the direction of $\mathbf{\Omega}$ the spin is stationary. If the spin orientation $\mathbf{s}$ deviates from the direction of $\mathbf{\Omega}$, for example by the angle ζ, then the spin precesses clockwise about the $\mathbf{\Omega}$-axis with the frequency Ω.

exchange spin field $-\omega_B\widehat{\phi}$ form an effective spin field $\mathbf{\Omega} = \omega_e\widehat{\mathbf{z}} - \omega_B\widehat{\phi} = \vec{\omega}_e + \vec{\omega}_B$ that is stationary in the orbiting and spinning system S. When the spin is aligned parallel or antiparallel to $\mathbf{\Omega}$ it is in a stationary state in the system S. Otherwise the spin precesses clockwise (cw) about the spin field axis $\widehat{\mathbf{\Omega}}$ with the frequency Ω.

Another important result of the classical calculation is that the magnetic energy of the electrons is reduced from the usual value $-\mu_B B_0$ where B_0 is the exchange field of the magnetization in the nanotube.

In the current paper we examine the quantum mechanical treatment of this problem. In our calculation we use a few simplifications that have no effect on the results: (a) a nanotube is used with zero wall thickness. Then the nanotube is a two-dimensional cylindrical surface with a circumference of $2\pi R$ and length L. (b) We ignore the velocity v_z of the electrons in the z-direction. The only effect of v_z is to reduce the value of $v_\phi = \pm\sqrt{v_F^2 - v_z^2}$, where v_F is the Fermi velocity. In addition, we assume an infinite mean free path of the electrons (which is not a trivial experimental challenge).

2 Quantum theoretical calculation

The potential energy of an electron spin in a magnetic field is $U = -\vec{\mu}\cdot\mathbf{B} = \mathbf{s}\cdot\vec{\omega}_\mathbf{B}$. But when the electron passes through regions with different magnetic field orientations then the interplay of torque and precession is no longer able to align the spin parallel to the magnetization and to optimize the potential energy. In the case in which we are interested, an electron in a circular magnetic nanotube, the electron must possess eigenstates that combine the orbital and the spin state. However, the interaction of an electron spin with its orbital motion can be rather complicated if one wants to go the traditional path: constructing a Lagrangian for angular rotational motion including spin and deriving a Hamiltonian from the Lagrangian.

Usually a different approach is taken by going into a system that moves with electron. A well-known example is the calculation of the spin-orbit interaction (see for example [19]). In our case we have an additional choice: the orientation of the axes in the moving frame which we denote as $(\widehat{\mathbf{x}}, \widehat{\mathbf{y}})$.

In the present paper we use two different approaches for the moving system. They are sketched in Figure 2, which shows a cross section through the nanotube perpendicular to the z-axis. Both coordinate systems have the same z-axis. The position of the electron (at the dot on the circumference in Fig. 2) is given in the system $(\widehat{\mathbf{x}}_0, \widehat{\mathbf{y}}_0)$ by the angle ϕ. The spin function, i.e., the spin orientation is measured in the coordinate system $(\widehat{\mathbf{x}}, \widehat{\mathbf{y}})$.

Lab system

In Figure 2a the orientation of the axes are the same: $(\widehat{\mathbf{x}}, \widehat{\mathbf{y}}) = (\widehat{\mathbf{x}}_0, \widehat{\mathbf{y}}_0)$. In the lab system the spin function $\chi(\phi, t)$ of a single electron is a function of ϕ and t. For the discussion we choose the position ϕ marked by the dot. The electron moves with the angular velocity ω_e counterclockwise (ccw) along the circumference of the cylinder. The magnetic field at the position $\mathbf{r} = (R, \phi, z)$ depends only on ϕ in this coordinate system.

$$\mathbf{B} = B_0\,(-\sin\phi, \cos\phi, 0)\,.$$

Orbiting system

In Figure 2b an orbiting coordinate system is used that moves with the electron with the angular velocity ω_e. The angle ϕ_o (o for orbiting) denotes a position in the orbiting system. An electron that starts at $t = 0$ from the position $\phi_o = \phi$ propagates in the finite time t to the position in the lab system at ϕ with

$$\phi = \phi_o + \omega_e t.$$

The magnetic field in the orbiting system becomes time dependent. The spin orientation is measured in the coordinate system $(\widehat{\mathbf{x}}, \widehat{\mathbf{y}})$ which is parallel to $(\widehat{\mathbf{x}}_0, \widehat{\mathbf{y}}_0)$. When we have determined the spin function $\overline{\chi}(\phi_o, t)$ in the orbiting system then it can be transformed back into the lab system. This orbiting system is actually the frame in which Thomas determined the relativistic spin-orbit interaction [19].

Orbiting and spinning system

In Figure 2c the coordinates $(\mathbf{x}, \mathbf{y})$ orbit as in Figure 1b. The electron position is given by ϕ_o, the same as in the orbiting system. In addition, the coordinate system $(\widehat{\mathbf{x}}, \widehat{\mathbf{y}})$ of the spin space is also rotated ccw by $\omega_e t$. As a consequence $\widehat{\mathbf{y}}$ is parallel to the tangent at the position $\mathbf{r}$ of the

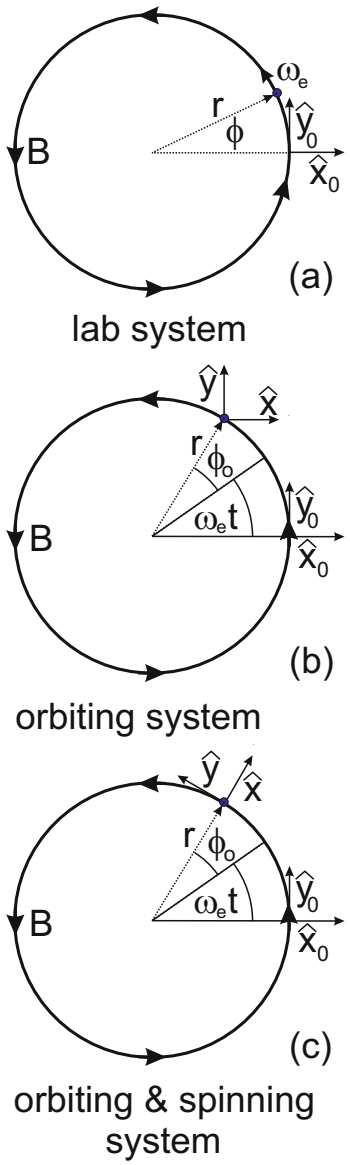

Fig. 2. A cross section through the nanotube. The electron orbits along the circumference with the angular velocity ω_e. (a) The coordinate axes are fixed in the lab system. (b) The coordinate axes $(\hat{\mathbf{x}}, \hat{\mathbf{y}})$ of the spin in the orbiting system are kept parallel to the axes $(\hat{\mathbf{x}}_0, \hat{\mathbf{y}}_0)$ of the lab system. (c) The coordinate axes $(\hat{\mathbf{x}}, \hat{\mathbf{y}})$ of the spin in the orbiting and spinning system spin with frequency ω_e so that $\hat{\mathbf{y}}$ is parallel to the tube circumference. In this system the magnetic field $\mathbf{B}$ points in the $\hat{\mathbf{y}}$ direction.

electron. Therefore one obtains the same magnetic field for every ϕ_o in this coordinate frame

$$\mathbf{B} = B_0 \hat{\mathbf{y}}.$$

When the spin function is determined in this orbiting-spinning system $\tilde{\chi}(\phi_o, t)$ then the spin function can be rotated back into the lab system $(\hat{\mathbf{x}}_0, \hat{\mathbf{y}}_0)$.

In the orbiting system one obtains a time-dependent Hamiltonian. In the orbiting and spinning system one obtains an inertial torque in addition to the exchange field torque acting on the spin. We include both torques together to construct a potential energy of the spin in this system, and the resulting Hamiltonian for the spin function can be easily solved. Finally one has to transform both results back into the lab system.

2.1 Thomas precession

Since the electron experiences acceleration along its path on the cylindrical surface one has to consider in principle relativistic effects, including the Thomas precession [19]. We estimated the magnitude of the Thomas precession in our classical calculation [18] for an electron with the Fermi velocity of 10^6 m/s. The resulting Thomas precession was several orders of magnitude smaller than the effects predicted here. Therefore, we can neglect it in our present calculation.

2.2 Electron propagation in the orbiting system

In our first approach we use the orbiting coordinate system as shown in Figure 2b. Here the spin frame $(\hat{\mathbf{x}}, \hat{\mathbf{y}})$ is parallel to the lab frame $(\hat{\mathbf{x}}_0, \hat{\mathbf{y}}_0)$. We consider the electron at the position (R, ϕ_o, z) (the properties depend only on ϕ_o). The corresponding position in the lab system is given by $\phi = \phi_o + \omega_e t$. The magnetic field in the orbiting system is

$$\mathbf{B} = B_0 \left(-\sin\left(\phi_o + \omega_e t\right), \cos\left(\phi_o + \omega_e t\right), 0\right).$$

2.2.1 Hamiltonian

The potential energy of the electron's magnetic moment $\vec{\mu}$ in the magnetic field is

$$U = -\vec{\mu}\cdot\mathbf{B} = -\gamma_e \mathbf{s}\cdot\mathbf{B} = \frac{2\mu_B}{\hbar}\mathbf{s}\cdot\mathbf{B} = \mu_B \vec{\sigma}\cdot\mathbf{B}, \quad (2)$$

where $\gamma = -g\mu_B/\hbar = -2\mu_B/\hbar$ is the gyromagnetic ratio, g is set to $g = 2$, and $\vec{\sigma} = (\sigma_x, \sigma_y, \sigma_z)$ are the Pauli matrices.

The resulting Hamiltonian has the form

$$H = \mu_B B_0 \begin{pmatrix} 0 & -i\exp\left[-i\left(\phi_o + \omega_e t\right)\right] \\ i\exp\left[i\left(\phi_o + \omega_e t\right)\right] & 0 \end{pmatrix}. \quad (3)$$

The time-dependent Schrödinger equation for the spin $\overline{\chi} = (\alpha, \beta)^T$ takes the form

$$i\hbar \begin{pmatrix} \mathring{\alpha} \\ \mathring{\beta} \end{pmatrix} = \mu_B B_0 \times \begin{pmatrix} 0 & -i\exp\left[-i\left(\phi_o + \omega_e t\right)\right] \\ i\exp\left[i\left(\phi_o + \omega_e t\right)\right] & 0 \end{pmatrix} \times \begin{pmatrix} \alpha \\ \beta \end{pmatrix}. \quad (4)$$

We make the ansatz

$$\alpha(t) = \alpha_0 \exp(-i\omega_\alpha t),$$
$$\beta(t) = \beta_0 \exp(-i\omega_\beta t).$$

After a short calculation one obtains

$$\hbar\omega_\alpha\alpha_0 = -i\beta_0\mu_B B_0 \exp\left[i\left(-\phi_o - (\omega_e - \omega_\alpha + \omega_\beta)t\right)\right], \quad (5)$$
$$\hbar\omega_\beta\beta_0 = i\alpha_0\mu_B B_0 \exp\left[i\left(\phi_o + (\omega_e - \omega_\alpha + \omega_\beta)t\right)\right].$$

Since the left side is time independent one has to require

$$(\omega_e - \omega_\alpha + \omega_\beta) = 0 \quad (6)$$

yielding

$$\hbar\omega_\alpha\alpha_0 = -i\beta_0\mu_B B_0 \exp(-i\phi_o), \quad (7)$$
$$\hbar\omega_\beta\beta_0 = i\alpha_0\mu_B B_0 \exp(i\phi_o).$$

Then equations (7) yield

$$\alpha_0 = -i\beta_0 \frac{\mu_B B_0 \exp(-i\phi_o)}{\hbar\omega_\alpha},$$
$$\beta_0 = i\alpha_0 \frac{\mu_B B_0 \exp(i\phi_o)}{\hbar\omega_\beta},$$
$$\hbar\omega_\alpha\hbar\omega_\beta = \mu_B^2 B_0^2. \quad (8)$$

Equations (6) and (8) yield the frequencies ω_α and ω_b. Setting

$$\hbar\omega_B = 2\mu_B B_0, \quad \Omega = \sqrt{\omega_e^2 + \omega_B^2} \quad (9)$$

one obtains

$$\omega_a = \frac{1}{2}\omega_e \pm \frac{1}{2}\Omega, \quad (10)$$
$$\omega_\beta = -\frac{1}{2}\omega_e \pm \frac{1}{2}\Omega. \quad (11)$$

Using the identity

$$\omega_B^2 = \Omega^2 - \omega_e^2 = (\Omega + \omega_e)(\Omega - \omega_e)$$

one can write the eigenvectors of the Hamiltonian.

2.2.2 Solution in orbiting system without spinning

For the first solution with the plus sign in equations (10) and (11) one obtains

$$\alpha_0 = -i\beta_0 \frac{\omega_B}{\Omega + \omega_e} \exp(-i\phi_o),$$
$$\beta_0 = i\alpha_0 \frac{\omega_B}{\Omega - \omega_e} \exp(i\phi_o),$$
$$|\alpha_0|^2 = \frac{1}{2\Omega}\frac{(\Omega - \omega_e)^2}{\Omega - \omega_e} = \frac{1}{2\Omega}(\Omega - \omega_e),$$
$$\alpha_0 = \frac{1}{\sqrt{2\Omega}}\sqrt{(\Omega - \omega_e)} \exp(-i\phi_o/2),$$
$$\beta_0 = i\frac{1}{\sqrt{2\Omega}}\sqrt{\Omega + \omega_e} \exp(i\phi_o/2),$$
$$\overline{\chi}_1(\phi_o, t) = \begin{pmatrix} \alpha_1(t) \\ \beta_1(t) \end{pmatrix} = \frac{1}{\sqrt{2\Omega}} \begin{pmatrix} \sqrt{(\Omega - \omega_e)} \exp\left[-\frac{i}{2}\omega_e t - \frac{i}{2}\phi_o\right] \\ i\sqrt{(\Omega + \omega_e)} \exp\left[+\frac{i}{2}\omega_e t + \frac{i}{2}\phi_o\right] \end{pmatrix} \times \exp\left(-\frac{i}{2}\Omega t\right). \quad (12)$$

Similarly

$$\overline{\chi}_2(\phi_o, t) = \begin{pmatrix} \alpha_2(t) \\ \beta_2(t) \end{pmatrix} = \frac{1}{\sqrt{2\Omega}} \begin{pmatrix} i\sqrt{(\Omega + \omega_e)} \exp\left[-\frac{i}{2}\omega_e t - \frac{i}{2}\phi_o\right] \\ \sqrt{\Omega - \omega_e} \exp\left[+\frac{i}{2}\omega_e t + \frac{i}{2}\phi_o\right] \end{pmatrix} \times \exp\left(\frac{i}{2}\Omega t\right). \quad (13)$$

2.2.3 Lab system

The axes $(\widehat{\mathbf{x}}, \widehat{\mathbf{y}})$ for the spin in the orbiting system are parallel to the axes $(\widehat{\mathbf{x}}_0, \widehat{\mathbf{y}}_0)$ in the lab system. Since the electron propagates on the cylinder with the angular velocity ω_e the term $\omega_e t$ is equivalent to the angle $\omega_e t = \phi - \phi_o$ on the cylinder.

Replacing $\omega_e t$ by $(\phi - \phi_o)$ in equations (12) and (13) yields the spin functions $\chi_1(\phi, t)$ and $\chi_2(\phi, t)$ in the lab system

$$\chi_1(\phi, t) = \frac{1}{\sqrt{2\Omega}} \begin{pmatrix} \sqrt{(\Omega - \omega_e)} \exp\left(-\frac{i}{2}\phi\right) \\ i\sqrt{(\Omega + \omega_e)} \exp\left(\frac{i}{2}\phi\right) \end{pmatrix} \exp\left(-\frac{i}{2}\Omega t\right), \quad (14)$$

$$\chi_2(\phi, t) = \frac{1}{\sqrt{2\Omega}} \begin{pmatrix} i\sqrt{(\Omega + \omega_e)} \exp\left(-\frac{i}{2}\phi\right) \\ \sqrt{\Omega - \omega_e} \exp\left(\frac{i}{2}\phi\right) \end{pmatrix} \exp\left(\frac{i}{2}\Omega t\right). \quad (15)$$

The expectation value of the magnetic energy is

$$\begin{aligned} E_i &= \langle \chi_i(\phi) | \mu_B \vec{\sigma}\cdot\mathbf{B} | \chi_i(\phi) \rangle \\ &= \frac{1}{2}\hbar\omega_B \langle \chi_i(\phi,t)| \\ &\quad \times \begin{pmatrix} 0 & -i\exp(-i\phi) \\ i\exp(+i\phi) & 0 \end{pmatrix} |\chi_i(\phi,t)\rangle \\ E_{1,2} &= \pm\frac{1}{2}\frac{\hbar\omega_B^2}{\Omega}. \end{aligned} \tag{16}$$

2.2.4 Eigenoperator of the spin state

In our classical derivation [18] it was shown that the electron experiences an effective magnetic field $\mathbf{B}_{\text{eff}}$ where

$$\mathbf{B}_{\text{eff}} = \mathbf{B} + \frac{1}{\gamma}\vec{\omega}_e = \frac{1}{\gamma}\mathbf{\Omega} \tag{17}$$

is composed of the actual exchange field $\mathbf{B}$ and an inertial field $\vec{\omega}_e/\gamma_e$. To calculate the component of the Pauli matrix vector $\vec{\sigma}$ in the local direction of $\mathbf{B}_{\text{eff}}$ we define $\mathbf{n}$ as

$$\mathbf{n} = \widehat{\mathbf{B}}_{\text{eff}} = \frac{1}{\Omega}(-\omega_B\sin\phi, \omega_B\cos\phi, -\omega_e). \tag{18}$$

Then we obtain

$$\sigma_{\mathbf{n}} = \mathbf{n}\cdot\vec{\sigma} = \begin{pmatrix} -\omega_e & -i\omega_B\exp(-i\phi) \\ i\omega_B\exp(i\phi) & \omega_e \end{pmatrix}.$$

We apply the operator $\sigma_{\mathbf{n}}$ to the spin state $\chi_1(\phi)$

$$\begin{aligned} \sigma_{\mathbf{n}}\chi_1(\phi) &= \frac{1}{\Omega}\begin{pmatrix} -\omega_e & -i\omega_B\exp(-i\phi) \\ i\omega_B\exp(i\phi) & \omega_e \end{pmatrix}\chi_1(\phi) \\ &= -\frac{1}{\sqrt{2\Omega}}\frac{1}{\Omega} \\ &\quad \times \begin{pmatrix} \sqrt{\Omega-\omega_e}\left(\omega_e - \omega_B\frac{\sqrt{\omega_e+\Omega}}{\sqrt{\Omega-\omega_e}}\right)e^{-\frac{1}{2}i\phi} \\ -i\sqrt{\omega_e+\Omega}\left(\omega_e + \omega_B\frac{\sqrt{\Omega-\omega_e}}{\sqrt{\omega_e+\Omega}}\right)e^{\frac{1}{2}i\phi} \end{pmatrix}. \end{aligned}$$

Using

$$\begin{aligned} \omega_B &= \sqrt{(\Omega-\omega_e)(\Omega+\omega_e)} \qquad \text{yields} \\ &= \frac{1}{\sqrt{2\Omega}}\begin{pmatrix} \sqrt{\Omega-\omega_e}e^{-\frac{1}{2}i\phi} \\ i\sqrt{\omega_e+\Omega}e^{\frac{1}{2}i\phi} \end{pmatrix} = \chi_1(\phi). \end{aligned}$$

The result

$$\sigma_{\mathbf{n}}\chi_1(\phi) = \chi_1(\phi)$$

shows that $\chi_1(\phi)$ is an eigenstate of $\sigma_{\mathbf{n}}$ with the eigenvalue one. Similarly $\chi_2(\phi)$ is an eigenstate of $\sigma_{\mathbf{n}}$ with the eigenvalue -1.

2.3 Electron in orbiting and spinning system S

For the derivation in the orbiting system we followed an electron along its orbit as a function of time. This means that at any given time t we considered the electron at the specific position (R, ϕ_o, z). This is a rather classical approach. Only after solving the Schrödinger equation did we split the time dependence into a (ϕ, t)-dependence in the lab system.

To demonstrate that this yields the correct wave function we perform a second derivation where we treat the electron spin in the frame S which orbits together with the electron with the angular velocity ω_e (as before), but whose spin frame $(\widehat{\mathbf{x}}, \widehat{\mathbf{y}}, \widehat{\mathbf{z}})$ is kept parallel to the unit vectors of the cylinder $(\widehat{\mathbf{r}}, \widehat{\boldsymbol{\phi}}, \widehat{\mathbf{z}})$. This means that the axes of the electron frame S are spinning with respect to lab frame S_0 with the angular velocity $\vec{\omega}_e$. The unit vectors of the lab frame are $(\widehat{\mathbf{x}}_0, \widehat{\mathbf{y}}_0, \widehat{\mathbf{z}}_0)$. This is shown in Figure 2c. The frame S is the same that was used in our classical calculation [18]. For the frame S the potential energy is modified due an inertial torque. Then the Hamiltonian in the frame S with its new potential energy is time independent.

First we consider classically the electron spin in the frame S. The orientation of the spin $\mathbf{s}$ changes due to the facts: (a) that we are in a spinning system and (b) that the magnetic field creates a torque. The relation between $d\mathbf{s}/dt$ in the inertial system S_0 and the orbiting and spinning system S is given by (see for example [20])

$$\left(\frac{d\mathbf{s}}{dt}\right)_{S_0} = \left(\frac{d\mathbf{s}}{dt}\right)_S + \vec{\omega}_e \times \mathbf{s} \tag{19}$$

(the same approach is used to calculate the Coriolis and centrifugal force on earth). With $(d\mathbf{s}/dt)_{S_0} = \gamma\mathbf{s}\times\mathbf{B}$ in the inertial lab system one obtains in the system S a total $(d\mathbf{s}/dt)_S$ which corresponds to an effective torque $\vec{\tau}_{\text{eff}}$

$$\left(\frac{d\mathbf{s}}{dt}\right)_S = \mathbf{s}\times(\gamma\mathbf{B}+\vec{\omega}_e) = \gamma\mathbf{s}\times\mathbf{B}_{\text{eff}} = \vec{\tau}_{\text{eff}}.$$

Here we set

$$\mathbf{B}_{\text{eff}} = \frac{\omega_e}{\gamma}\widehat{\mathbf{z}} + B_0\widehat{\mathbf{y}}, \qquad \mathbf{\Omega} = \gamma\mathbf{B}_{\text{eff}} = \omega_e\widehat{\mathbf{z}} + \gamma B_0\widehat{\mathbf{y}}.$$

$\mathbf{B}_{\text{eff}}$ is a (local) effective field. In the system S it is constant and lies in the $\widehat{\mathbf{y}}$-$\widehat{\mathbf{z}}$-plane (which corresponds to $\widehat{\boldsymbol{\phi}}$-$\widehat{\mathbf{z}}$-plane in the lab system). The vector $\mathbf{\Omega}$ is anti-parallel to $\mathbf{B}_{\text{eff}}$. It is considered as a spin field. We define the angle between $\mathbf{\Omega}$ and the z-axis as α with

$$\tan\alpha = \frac{2\mu_B B_0}{\hbar\omega_e} = \frac{\omega_B}{\omega_e}.$$

The integration of $\vec{\tau}_{\text{eff}}$ yields the classical potential energy in the spinning system

$$U = -\vec{\mu}\cdot\mathbf{B}_{\text{eff}} = -\gamma\mathbf{s}\cdot\mathbf{B}_{\text{eff}} = -\mathbf{s}\cdot\mathbf{\Omega}.$$

Now we use the Hamiltonian $H = U$. The solution of the time-independent Schrödinger equation $H\widetilde{\chi} = E\widetilde{\chi}$ is

straight forward and yields the spin states in the system S with the eigenvalues $E = \pm\hbar\Omega/2 = \pm\hbar\sqrt{\omega_e^2 + \omega_B^2}/2$

$$\widetilde{\chi}_1(t) = \frac{1}{\sqrt{2\Omega}} \begin{pmatrix} \sqrt{\Omega - \omega_e} \\ i\sqrt{(\Omega + \omega_e)} \end{pmatrix} \exp\left(-\frac{i}{2}\Omega t\right), \quad (20)$$

$$\widetilde{\chi}_2(t) = \frac{1}{\sqrt{2\Omega}} \begin{pmatrix} i\sqrt{\Omega + \omega_e} \\ \sqrt{\Omega - \omega_e} \end{pmatrix} \exp\left(+\frac{i}{2}\Omega t\right). \quad (21)$$

In the system S the spin states $\widetilde{\chi}_1(t)$ and $\widetilde{\chi}_2(t)$ possess no angular dependence. This calculation has the advantage that it treats the position and time independently.

The ϕ-dependence of the spin state in the coordinates of the orbiting system is obtained by performing a spin rotation of the spin states in equations (20) and (21) by $(\phi_o + \omega_e t)$ about the z-axis. The general form for the rotation of angular momentum states $\mathbf{J}$ is

$$R(\vec{\eta}) = \exp(-i\mathbf{J}\cdot\vec{\eta}/\hbar),$$

where $\widehat{\eta}$ gives the axis of rotation and η is the angle of rotation. For spin 1/2 one has $\mathbf{J} = \frac{\hbar}{2}\vec{\sigma}$, and here $\vec{\eta} = (\phi_o + \omega_e t)\,\widehat{\mathbf{z}}$. This gives

$$R((\phi_o + \omega_e t)\,\widehat{\mathbf{z}}) = \begin{pmatrix} \exp(-i(\phi_o + \omega_e t)/2) & 0 \\ 0 & \exp(i(\phi_o + \omega_e t)/2) \end{pmatrix}.$$

$R\widetilde{\chi}_i$ yields the spin states $\overline{\chi}_i$ as given in equations (12) and (13) in the orbiting system. The transformation of the spin states from the orbiting system to the lab system is discussed in Section 2.2.3.

3 Discussion

3.1 Quantization direction

In our classical derivation [18] it was shown that the electron experiences an effective magnetic field $\mathbf{B}_{\text{eff}}$. If its spin is aligned parallel or antiparallel to $\mathbf{B}_{\text{eff}}$ the spin is stationary in the orbiting and spinning system S. Here

$$\mathbf{B}_{\text{eff}} = \mathbf{B} + \frac{1}{\gamma}\vec{\omega}_e$$

is composed of the actual exchange field $\mathbf{B}$ and an inertial field $\vec{\omega}_e/\gamma_e$. The corresponding spin field is given by $\mathbf{\Omega} = \gamma\mathbf{B}_{\text{eff}} = -2\mu_B\mathbf{B}_{\text{eff}}/\hbar$ and has the opposite direction.

In Section 2.2.4 we defined the component of the Pauli matrix vector $\mathbf{s}$ in the local direction of $\mathbf{B}_{\text{eff}}$ in the lab frame S_0 as $\sigma_{\mathbf{n}} = \mathbf{n}\cdot\vec{\sigma}$ with the unit vector $\mathbf{n} = \widehat{\mathbf{B}}_{\text{eff}}$ and showed for $\chi_1(\phi, t)$ that

$$\sigma_{\mathbf{n}}\chi_1(\phi, t) = \chi_1(\phi, t).$$

This demonstrates that $\chi_1(\phi, t)$ is an eigenstate of the (spin) operator $\sigma_{\mathbf{n}}$ with the eigenvalue 1. In other words the direction of $\mathbf{n} = \widehat{\mathbf{B}}_{\text{eff}} = -\widehat{\mathbf{\Omega}}$ is the direction of quantization. The state $\chi_1(\phi, t)$ is the local spin-up state with respect to $\widehat{\mathbf{B}}_{\text{eff}}$, and $\chi_2(\phi, t)$ is the corresponding spin-down state.

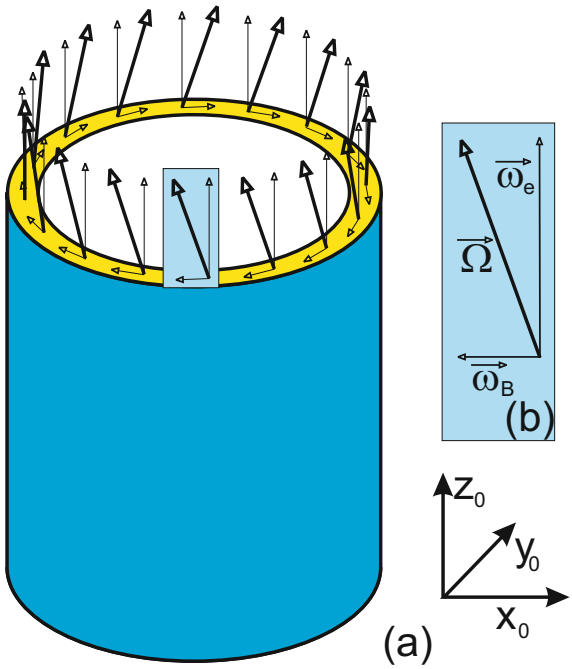

Fig. 3. (a) An electron circles the nanotube with ω_e in an exchange field of $\mathbf{B} = B_0\widehat{\phi}$. This figure shows the components $-\omega_B\widehat{\phi}$ and $\omega_e\widehat{\mathbf{z}}$ of the spin field $\mathbf{\Omega}$ in the nanotube in the lab system as thin circular and vertical arrows. (b) Shows the components of $\mathbf{\Omega}$ enlarged. The sum $\mathbf{\Omega} = -\omega_B\widehat{\phi} + \omega_e\widehat{\mathbf{z}}$ of the two components is the total spin field and is shown as thick arrows. Its unit vector $\widehat{\mathbf{\Omega}}$ gives the quantization direction. The expectation value of $\langle\vec{\sigma}\rangle$ is either $+\widehat{\mathbf{\Omega}}$ or $-\widehat{\mathbf{\Omega}}$ for the two eigenstates. $(\hbar\vec{\omega}_B = -2\mu_B B_0\widehat{\phi})$.

3.2 Spin expectation values

In Appendix A the expectation values of the spin, i.e. the Pauli matrices $\langle\sigma_x\rangle$, $\langle\sigma_y\rangle$ and $\langle\sigma_z\rangle$ for $\chi_1(\phi)$ and $\chi_2(\phi)$ are calculated. They are equal to the components of the unit vector of $\mathbf{\Omega}$, i.e. $\langle\vec{\sigma}\rangle = \pm\widehat{\mathbf{\Omega}}$ with the plus sign for $\chi_2(\phi)$.

In Figure 3 the components $-\omega_B\widehat{\phi}$ and $\omega_e\widehat{\mathbf{z}}$ of the spin field $\mathbf{\Omega}$ are shown as thin arrows on top of the nanotube. $\vec{\omega}_B = -\omega_B\widehat{\phi}$ is the component due to the magnetic exchange field and $\omega_e\widehat{\mathbf{z}}$ is the result of an inertial torque. The thick arrows represent $\mathbf{\Omega}$, which determines the direction of quantization for the spin states.

Interestingly we obtained the same components in the classical calculation. The important difference is, of course, that in the classical treatment the electron is at a given time only at one place, while in quantum treatment the electron and its spin are distributed over the volume of the nanotube.

3.3 The full wave function of the electron

In the absence of a magnetic field (and impurities) the momenta of the electrons on the two-dimensional cylindrical surface are quantized as

$$q_\phi = n_\phi\frac{1}{R}, \qquad q_z = n_z\frac{2\pi}{L},$$

where (q_z, q_ϕ) are the wave vectors in z- and ϕ-direction for a cylinder of length L and radius R with periodic boundary conditions in the z-direction.

In the presence of the circular magnetic field the spin functions $\chi_i(\phi,t)$

$$\chi_i(\phi,t) = \begin{pmatrix} \alpha_{0,i}\exp\left(-\frac{i}{2}\phi\right) \\ \beta_{0,i}\exp\left(+\frac{i}{2}\phi\right) \end{pmatrix} \exp\left(\mp\frac{i}{2}\Omega t\right)$$

change their sign after a full circle of 2π due to the factors $\exp(\pm\frac{i}{2}\phi)$ so that

$$\chi_i(2\pi,t) = -\chi_i(0,t).$$

This phase shift of π has to be absorbed by the quantization of q_ϕ, which is now

$$q_\phi = \frac{(2n_\phi+1)\pi}{2\pi R} = \left(n_\phi+\frac{1}{2}\right)\frac{1}{R}. \tag{22}$$

Then the full wave function of the electron on the two-dimensional cylindrical surface is

$$\psi(\phi,z) = \exp\left\{i\left[\left(n_\phi+\frac{1}{2}\right)\phi + n_z\frac{2\pi z}{L}\right]\right\} \times \begin{pmatrix} \alpha_{0,i}\exp\left(-\frac{i}{2}\phi\right) \\ \beta_{0,i}\exp\left(+\frac{i}{2}\phi\right) \end{pmatrix}.$$

The quantization in the $\mathbf{\Omega}$ direction should be valid even if the circular magnetic field is very small.

3.4 Quantum theoretical precession

For a spin 1/2 particle one observes precession when the spin state is a superposition of the two spin eigenstates and these states have different frequencies. In our case the precessing spin function has the form

$$\chi(\phi,t) = A\chi_1(\phi,t) + B\chi_2(\phi,t). \tag{23}$$

We define the precession angle, the angle between the spin $\mathbf{s}$ and $\mathbf{\Omega}$, as ζ. We set $A = \sin(\zeta/2)$ and $B = \cos(\zeta/2)e^{i\delta}$. The phase δ determines the initial orientation of the spin. The spin function $\chi(\phi,t)$ is normalized, $|A|^2 + |B|^2 = 1$.

$$A = \sin(\zeta/2), \quad B = \cos(\zeta/2)\,e^{i\delta},$$
$$|B|^2 - |A|^2 = \cos\zeta, \quad 2AB = \sin\zeta e^{i\delta}. \tag{24}$$

In addition, the angle between $\mathbf{\Omega}$ and the z-axis is defined as α. In terms of α and ϕ the unit vector of the total spin field $\mathbf{\Omega}$ is

$$\widehat{\mathbf{\Omega}} = (\sin\alpha\sin\phi, -\sin\alpha\cos\phi, \cos\alpha). \tag{25}$$

The spin expectation value becomes

$$\begin{aligned}\langle\sigma_x(\phi,t)\rangle &= \langle\chi(\phi,t)|\sigma_x|\chi(\phi,t)\rangle \\ &= \sin^2(\zeta/2)\langle\chi_1(\phi,t)|\sigma_x|\chi_1(\phi,t)\rangle \\ &\quad + \cos^2(\zeta/2)\langle\chi_2(\phi,t)|\sigma_x|\chi_2(\phi,t)\rangle \\ &\quad + \frac{1}{2}\sin\zeta e^{i\delta}\langle\chi_1(\phi,t)|\sigma_x|\chi_2(\phi,t)\rangle \\ &\quad + \frac{1}{2}\sin\zeta e^{-i\delta}\langle\chi_2(\phi,t)|\sigma_x|\chi_1(\phi,t)\rangle.\end{aligned}$$

The diagonal matrix elements are time independent, but the off-diagonal ones oscillate with the energy difference between the two spin eigenstates. In Appendix A the matrix elements are calculated, and in Appendix B the time-independent and time-dependent expectation values of the spin are calculated. The results of this calculation are collected below. The time-independent parts of $\langle\vec{\sigma}\rangle$ are

$$\begin{aligned}\langle\sigma_x\rangle_0 &= \cos\zeta\sin\alpha\sin\phi \\ \langle\sigma_y\rangle_0 &= -\cos\zeta\sin\alpha\cos\phi \\ \langle\sigma_z\rangle_0 &= \cos\zeta\cos\alpha\end{aligned} \tag{26}$$

and the time-dependent parts are

$$\begin{aligned}\langle\sigma_x\rangle_t &= \sin\zeta\left[\cos\phi\cos(\Omega t+\delta) + \cos\alpha\sin\phi\sin(\Omega t+\delta)\right], \\ \langle\sigma_y\rangle_t &= \sin\zeta\left[\sin\phi\cos(\Omega t+\delta) - \cos\alpha\cos\phi\sin(\Omega t+\delta)\right], \\ \langle\sigma_z\rangle_t &= -\sin\zeta\sin\alpha\sin(\Omega t+\delta).\end{aligned} \tag{27}$$

The expectation values of the time-dependent part $\langle\vec{\sigma}\rangle_t$ and the time-independent part $\langle\vec{\sigma}\rangle_0$ are orthogonal to each other $\langle\vec{\sigma}\rangle_0 \cdot \langle\vec{\sigma}\rangle_t = 0$. By setting $\delta = \pi/2$ the spin expectation value of $\langle\vec{\sigma}\rangle$ at $t = 0$ lies in the plane spanned by $\widehat{\mathbf{z}}$ and $\vec{\omega}_B$, which is the tangential plane to the cylinder at ϕ (as do $\langle\vec{\sigma}\rangle_t$, $\langle\vec{\sigma}\rangle_0$, $\vec{\omega}_e$, and $\mathbf{\Omega}$). We use this value of δ in the following figures.

Equations (26) show that the constant component of the spin is just equal to the spin in the state $\chi_1(\phi)$ multiplied by the cosine of the precession angle $\cos\zeta$. This is a very intuitive result. It yields the expectation values of the eigenstates for $\zeta = 0$ and $\zeta = \pi$.

The time-dependent part of the spin expectation value precesses locally everywhere with the frequency Ω. The total z-component oscillates between the maximum value of $\cos\zeta\cos\alpha + \sin\zeta\sin\alpha = \cos(\alpha-\zeta)$ and the minimum value $\cos\zeta\cos\alpha - \sin\zeta\sin\alpha = \cos(\alpha+\zeta)$. These are the z-components of a spin that forms the angles of $\alpha\pm\zeta$ with the z-axis. That is exactly what one expects if the spin moves along a cone about $\mathbf{\Omega}$ with an angle of ζ. The same applies to the x- and y-components of the spin. So locally the spin precesses everywhere in the nanotube about the local quantization direction $\mathbf{\Omega}$ with the constant precession angle ζ and the precession frequency Ω.

The precession is shown in Figure 4 in detail. Figure 4a shows a cross section through the nanotube. The precession cones are shown for $\phi = 0, \pi/2, \pi$ and $3\pi/2$. The cones are locally rigid. Only the spin precesses. In Figure 4b such a cone is shown enlarged. Its axis is the effective spin field $\mathbf{\Omega}$, which is inclined in the direction of the local field $\vec{\omega}_B$, ($\vec{\omega}_B = -\omega_B\widehat{\phi}$). The angle of the cone, i.e. the angle between $\mathbf{\Omega}$ and $\mathbf{s}$, is ζ. On the upper circular surface the end point of the spin $\mathbf{s}$ is shown. One recognizes the local angle of precession Ωt on the circular surface of the cone at the time t. If one attaches all cones rigidly to the circumference of the nanotube and rotates the nanotube plus cones like a carousel (for example by $\pi/2$) then one obtains the same figure.

We believe that one obtains an optimal insight into the precession if one draws the different cones in space as well as in time. This is done in Figure 5.

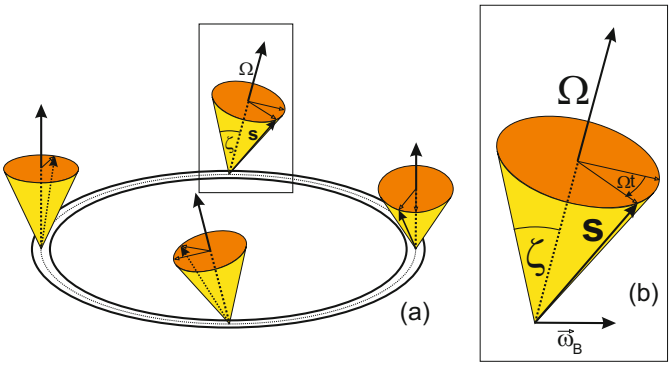

Fig. 4. The precession of the spin shown on a cross section of the nanotube. In part (b) the precession cone in the box is enlarged. The local precession axis $\mathbf{\Omega}$ is drawn. The precession cone has an angle of ζ between $\mathbf{\Omega}$ and the spin $\mathbf{s}$. The spin circles on the cone with angle Ωt. The corresponding cones at different positions can be easily constructed by attaching the cone rigidly to the cross section of the nanotube and then rotating the tube with the cone about the z-axis to the new position.

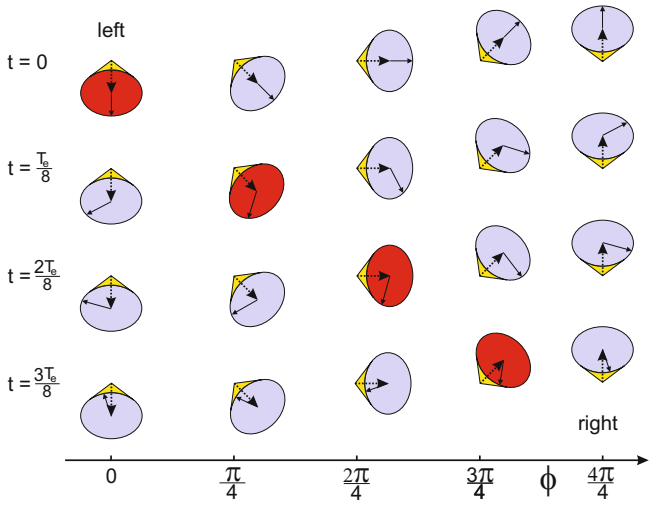

Fig. 5. The precession cone of the spin in the quantum theoretical treatment in an eagle-eye view from the top at different positions and times (see Fig. 4b). The horizontal axis gives the position along half of the circumference in steps of $\pi/4$. The time is shown on vertical axis in steps of $T_e/8 = \pi/(4\omega_e)$. The top row shows the cones at $t = 0$. The thick arrows are the axes of the cones and represent the time-independent part of the spin. The thin arrows represent the time-dependent part of the spin. The spin is the sum of the two arrows. In each time step Δt each thin arrow progresses by $\Omega\Delta t$. The cones with the red (dark) circular surfaces progress in time and space with the angular velocity ω_e of the electron and yield a relatively small effective precession in the orbiting system.

3.5 Comparison between the classical and the quantum theoretical calculations

The theoretical results for the precession in the classical calculation (CC) and the quantum theoretical calculation (QTC) agree in several essential points. In both calculations a specific direction $\mathbf{n}(\phi)$ emerges which is the same in CC and QTC and given by equation (18). The unit vector $\mathbf{n}(\phi)$ is parallel to $\mathbf{B}_{\text{eff}}$, antiparallel to $\mathbf{\Omega} = \gamma\mathbf{B}_{\text{eff}} = \vec{\omega}_B + \vec{\omega}_e$ and forms the constant angle α with the z-axis. In the QTC $\mathbf{n}(\phi)$ gives the direction of quantization, and in the CC $\mathbf{n}(\phi)$ gives the direction of the two stationary states. When the spin is aligned parallel or antiparallel to $\mathbf{n}(\phi)$ there is no precession, neither in CC nor in QTC. Precession is obtained when the spin forms a finite angle ζ with the direction of $\mathbf{n}(\phi)$. In Appendix C the detailed motion of the spin in CC is described.

In Figure 5 the precession cones are drawn for the QTC in an eagle-eye view from the top at different times and as a function of the angle along the circumference. The horizontal axis is the angle ϕ. The top row shows the cones at $t = 0$ for four angles: $\phi = 0, \pi/4, 2\pi/4, 3\pi/4$, and $4\pi/4$. This represents half a circumference. The ϕ-axis is shown as the horizontal axis to allow a better comparison at different times. The orientation of the cones is the same as on the nanotube at the corresponding angle.

We first discuss precession cones in the top row at $t = 0$. The thick arrows represent the axis of the cone with the direction of $\mathbf{\Omega}$. The thin arrows from the center of the circle to the rim of the cone point to the end of the spin arrows (compare Fig. 4b). The spin expectation $\langle\vec{\sigma}\rangle$ is essentially given by equations (26) and (27). Going from the left to the right each cone is rotated with respect to the previous cone by $\Delta\phi = \pi/4$ about the z-axis.

The different rows are redrawn for increasing time (going down) with $\Delta t = T_e/8$ where $T_e = 2\pi/\omega_e$ is the period for the electron to circle the nanotube one time. We follow the cones for a given column in time steps of $\Delta t = T_e/8$. The orientation of the cone is not altered but the spin has precessed around the cone axis with each Δt by $\Omega\Delta t = \Omega T_e/4$. So each column yields the local precession of the electron spin.

Figure 5 is well-suited to compare the classical precession with the quantum theoretical one. In the classical picture the electron is point-like and circles the nanotube with ω_e. Now we follow the cones along the diagonal from $t = 0$ to $t = T_e/8$. During this time the electron has propagated from the angle $\phi = 0$ to $\pi/4$. So it moves in Figure 5 from the top left $(1, 1)$ position diagonally to the $(2, 2)$ position corresponding to the angular velocity of $\Delta\phi/\Delta t = (\pi/4)/(T_e/8) = 2\pi/T_e = \omega_e$. This means that the cones along the diagonal in Figure 5 (with the red (dark) circular surfaces) represent the classical motion of an electron around the nanotube.

During the time $T_e/8$ the electron orbits ccw just the angle $\pi/4$ on the nanotube, i.e. it travels from one red cone to the next one. This next red cone has a different orientation by $\pi/4 = \omega_e T_e/4$, i.e. the angle of the spin field $\mathbf{\Omega}$ at this next red cone is rotated counter-clockwise by $\pi/4$ or 45°. In addition, the spin direction has precessed about the $\mathbf{\Omega}$-axis clockwise by $\Omega T_e/8$ (in Fig. 5 we use $\Omega T_e/8 = -55°$). Therefore the two rotations partially cancel each other. The result is a wobbly precession

because the z-component of the spin is not constant. For small ω_B the z- and $\mathbf{\Omega}$-axes are almost parallel, and the effective precession frequency is in good approximation given by the difference

$$\omega_{pcn} \approx \Omega - \omega_e = \sqrt{\omega_e^2 + \omega_B^2} - \omega_e \approx \frac{1}{2}\frac{\omega_B^2}{\omega_e}.$$

If one follows the red precession cones in Figure 5 then one moves with the angular velocity ω_e, the angular velocity of the electron. In this orbiting system the QTC yields the identical result for the expectation value of the spin $\langle \mathbf{s} \rangle$ as a function of time as in the CC (where one always moves with the electron). The latter is shown in Appendix C. The classical x- and y-components of the spin are plotted in Figures C.1 to C.3. The same plots give the expectation values $\langle s_x \rangle$ and $\langle s_y \rangle$ in the quantum theoretical calculation when moving with the electron.

However, this is not the traditional way how precession is defined in a quantum system. Instead one considers ϕ and t as independent variables and follows the precession at a constant position ϕ as a function of time. This is shown in the vertical columns in Figure 5. For constant ϕ this precession frequency is Ω.

4 Conclusion

Our quantum theoretical calculation confirms the results of the classical calculation: The spin of the conduction electrons does not align parallel or anti-parallel to the magnetization. Instead the quantization direction $\mathbf{n}_\sigma = \widehat{\mathbf{B}}_{\text{eff}} = -\widehat{\mathbf{\Omega}}$ has a dominant component parallel or anti-parallel to the z-axis of the tube. The magnitude of this component is proportional to the angular velocity of the electron $\vec{\omega}_e = (v_\phi/R)\widehat{\mathbf{z}}$. The other component of $\mathbf{n}_\sigma$ is parallel and proportional to the spin field of the magnetization $\omega_B\widehat{\phi}$. As a consequence $\mathbf{n}_\sigma$ depends on the position given by the angle ϕ, and the spin function changes sign around a closed loop with $\Delta\phi = 2\pi$. This alters the quantization condition for angular momentum.

This unusual spin alignment has a number of interesting effects that modify the band structure and magnetic properties [18]: (i) the ground-state energy of the circular magnetic state is increased, which will result in a reduction of the Curie temperature. (ii) This effect should be particularly important for Stoner magnets because in a one-band Stoner magnet there is a large feedback between the total electron spin and the magnetization. (iii) The interaction of the conduction electrons with the spin waves of a circular magnetic nanotube should be particularly interesting. A comparison of the electron-spin-wave interactions between a circular magnetic nanotube and a thin ferromagnetic film of the same material will yield interesting insight into the role of the relative polarization of the conduction electrons and the magnetization.

Author contribution statement

J.L. initiated the research project on ferromagnetic nanotubes. G.B. proposed the original idea of this paper. G.B. and R.T. performed the calculations.

The authors thank Dr. Ilya Krivorotov for helpful discussions. This work was partially supported by NSF Grant ECCS-1309416.

Appendix A: Pauli matrix elements between the spin eigenstates

In Section 2, equations (14) and (15) give the eigenstates for an electron spin in a nanotube with circular magnetization in the lab frame S_0. For the following discussion it is useful to express these states in terms of the angle α between the spin field $\mathbf{\Omega}$ and the z-axis. This yields

$$\begin{aligned} \cos\alpha &= \omega_e/\Omega, \qquad & \sin\alpha &= \omega_B/\Omega, \\ \cos(\alpha/2) &= \sqrt{(\Omega+\omega_e)}/\sqrt{2\Omega}, & & \\ \sin(\alpha/2) &= \sqrt{(\Omega-\omega_e)}/\sqrt{2\Omega}. & & \end{aligned} \tag{A.1}$$

Then one obtains

$$\chi_1(\phi) = \begin{pmatrix} \sin(\alpha/2)\exp\left(-\frac{i}{2}\phi\right) \\ i\cos(\alpha/2)\exp\left(\frac{i}{2}\phi\right) \end{pmatrix},$$

$$\chi_2(\phi) = \begin{pmatrix} i\cos(\alpha/2)\exp\left(-\frac{i}{2}\phi\right) \\ \sin(\alpha/2)\exp\left(\frac{i}{2}\phi\right) \end{pmatrix}.$$

A.1 Diagonal matrix elements

We calculate $\langle \chi_1(\phi)|\sigma_x|\chi_1(\phi)\rangle$

$$\begin{aligned} &= \begin{pmatrix} \sin(\alpha/2)\exp\left(-\frac{i}{2}\phi\right) \\ i\cos(\alpha/2)\exp\left(\frac{i}{2}\phi\right) \end{pmatrix}^\dagger \begin{pmatrix} 0 & 1 \\ 1 & 0 \end{pmatrix} \\ &\quad \times \begin{pmatrix} \sin(\alpha/2)\exp\left(-\frac{i}{2}\phi\right) \\ i\cos(\alpha/2)\exp\left(\frac{i}{2}\phi\right) \end{pmatrix} \\ &= -2\left(\cos\frac{1}{2}\alpha\sin\frac{1}{2}\alpha\right)\sin\phi = -\sin\alpha\sin\phi. \end{aligned}$$

Similarly one obtains the spin expectation values for σ_y and σ_z and the expectation values of the Pauli matrix with respect to $\chi_2(\phi)$. The results are collected in equation (A.2)

$$\begin{aligned} \langle \chi_1(\phi)|\sigma_x|\chi_1(\phi)\rangle &= -\sin\alpha\sin\phi, \\ \langle \chi_2(\phi)|\sigma_x|\chi_2(\phi)\rangle &= \sin\alpha\sin\phi, \\ \langle \chi_1(\phi)|\sigma_y|\chi_1(\phi)\rangle &= \sin\alpha\cos\phi, \\ \langle \chi_2(\phi)|\sigma_y|\chi_2(\phi)\rangle &= -\sin\alpha\cos\phi, \\ \langle \chi_1(\phi)|\sigma_z|\chi_1(\phi)\rangle &= -\cos\alpha, \\ \langle \chi_2(\phi)|\sigma_z|\chi_2(\phi)\rangle &= \cos\alpha. \end{aligned} \tag{A.2}$$

The sum of the squares of the expectation values for both $\chi_1(\phi)$ and $\chi_2(\phi)$ is

$$\langle\sigma_x\rangle^2 + \langle\sigma_y\rangle^2 + \langle\sigma_z\rangle^2 = 1.$$

A.2 Off-diagonal matrix elements of precession

Next we calculate the Pauli matrix elements between $\chi_1(\phi,t)$ and $\chi_2(\phi,t)$. One obtains for

$$\begin{aligned}
&\langle\chi_2(\phi,t)|\sigma_x|\chi_1(\phi,t)\rangle \\
&\quad= \begin{pmatrix} i\cos(\alpha/2)\exp\left(-\frac{i}{2}\phi\right) \\ \sin(\alpha/2)\exp\left(\frac{i}{2}\phi\right)\end{pmatrix}^\dagger \begin{pmatrix}0&1\\1&0\end{pmatrix} \\
&\quad\times \begin{pmatrix} \sin(\alpha/2)\exp\left(-\frac{i}{2}\phi\right) \\ i\cos(\alpha/2)\exp\left(\frac{i}{2}\phi\right)\end{pmatrix} e^{-i\Omega t} \\
&\quad= \left(e^{i\phi}\cos^2\frac{1}{2}\alpha + e^{-i\phi}\sin^2\frac{1}{2}\alpha\right)e^{-i\Omega t} \\
&\quad= (\cos\phi + i\cos\alpha\sin\phi)\,e^{-i\Omega t}.
\end{aligned}$$

Similarly one obtains the spin expectation values for σ_y and σ_z.The results are collected in equation (A.3)

$$\begin{aligned}
\langle\chi_2(\phi,t)|\sigma_x|\chi_1(\phi,t)\rangle &= (\cos\phi + i\cos\alpha\sin\phi)\,e^{-i\Omega t} \\
\langle\chi_2(\phi,t)|\sigma_y|\chi_1(\phi,t)\rangle &= (\sin\phi - i\cos\alpha\cos\phi)\,e^{-i\Omega t} \\
\langle\chi_2(\phi,t)|\sigma_z|\chi_1(\phi,t)\rangle &= -i\sin\alpha e^{-i\Omega t}. \qquad \text{(A.3)}
\end{aligned}$$

Appendix B: Quantum theoretical precession

We consider the spin function

$$\chi(t) = A\chi_1(t) + B\chi_2(t) = \sin(\zeta/2)\chi_1(t) + \cos(\zeta/2)e^{i\delta}\chi_2(t).$$

If we define ζ as the angle between the spin direction and the $\mathbf{\Omega}$ axis, we can set $A = \sin(\zeta/2)$ and $B = \cos(\zeta/2)e^{i\delta}$. Then we get

$$|B|^2 - |A|^2 = \cos\zeta \qquad 2AB = \sin\zeta e^{i\delta}.$$

Next we calculate the spin expectation value

$$\begin{aligned}
\langle\sigma_x\rangle &= \langle\chi(t)|\sigma_x|\chi(t)\rangle \\
&= \sin^2(\zeta/2)\langle\chi_1(t)|\sigma_x|\chi_1(t)\rangle \\
&\quad + \cos^2\zeta\langle\chi_2(t)|\sigma_x|\chi_2(t)\rangle \\
&\quad + \frac{1}{2}\sin\zeta e^{i\delta}\langle\chi_1(t)|\sigma_x|\chi_2(t)\rangle \\
&\quad + \frac{1}{2}\sin\zeta e^{-i\delta}\langle\chi_2(t)|\sigma_x|\chi_1(t)\rangle.
\end{aligned}$$

Further we use that

$$\begin{aligned}
\langle\chi_1(t)|\sigma_x|\chi_2(t)\rangle &= \langle\chi_2(t)|\sigma_x|\chi_1(t)\rangle^* \\
&= \left(\cos\phi - i\frac{\omega_e}{\Omega}\sin\phi\right)e^{+i(\Omega t+\delta)}.
\end{aligned}$$

Using equations (A.2) and (A.3) gives

$$\begin{aligned}
\langle\sigma_x\rangle &= \sin^2(\zeta/2)(-\sin\alpha\sin\phi) + \cos^2\zeta\sin\alpha\sin\phi \\
&\quad + \frac{1}{2}\sin\zeta(\cos\phi - i\sin\alpha\sin\phi)\,e^{+i(\Omega t+\delta)} \\
&\quad + \frac{1}{2}\sin\zeta(\cos\phi + i\sin\alpha\sin\phi)\,e^{-i(\Omega t+\delta)}.
\end{aligned}$$

This yields

$$\begin{aligned}
\langle\sigma_x\rangle &= \cos\zeta\sin\alpha\sin\phi + \sin\zeta[\cos\phi\cos(\Omega t+\delta) \\
&\quad + \cos\alpha\sin\phi\sin(\Omega t+\delta)].
\end{aligned}$$

Similarly we obtain the expectation values of $\langle\sigma_y\rangle$ and $\langle\sigma_z\rangle$. Then we split the results into the time-independent parts

$$\begin{aligned}
\langle\sigma_x\rangle_0 &= \cos\zeta\sin\alpha\sin\phi, \\
\langle\sigma_y\rangle_0 &= -\cos\zeta\sin\alpha\cos\phi, \\
\langle\sigma_z\rangle_0 &= \cos\zeta\cos\alpha,
\end{aligned}$$

and the time-dependent parts

$$\begin{aligned}
\langle\sigma_x\rangle_t &= \sin\zeta\left[\cos\phi\cos(\Omega t+\delta) + \cos\alpha\sin\phi\sin(\Omega t+\delta)\right], \\
\langle\sigma_y\rangle_t &= \sin\zeta\left[\sin\phi\cos(\Omega t+\delta) - \cos\alpha\cos\phi\sin(\Omega t+\delta)\right], \\
\langle\sigma_z\rangle_t &= -\sin\zeta\sin\alpha\sin(\Omega t+\delta).
\end{aligned}$$

These equations are denoted as (27) and (26) in Section 4.1. Like for the eigenstates (A.2), one obtains for the time-dependent precession states

$$\langle\sigma_x\rangle^2 + \langle\sigma_y\rangle^2 + \langle\sigma_z\rangle^2 = 1.$$

Appendix C: Details of the classical precession

We recall briefly the dynamics of the CC, which is sketched in Figure 1. The electron is treated in the orbiting and spinning system S with local axes $(\widehat{\mathbf{x}},\widehat{\mathbf{y}})$ parallel to $(\widehat{\mathbf{r}},\widehat{\phi})$. In the stationary states the spin aligns parallel or antiparallel to the spin field $\mathbf{\Omega}$, which is the sum of $\vec{\omega}_B$ and $\vec{\omega}_e$, both shown in Figure 1. In the lab system $\mathbf{\Omega}$ rotates with ω_e counterclockwise about the z-axis. Its angle with the z-direction is defined as α. If the spin is not aligned parallel to $\pm\mathbf{\Omega}$ then it precesses about the $\mathbf{\Omega}$ with the frequency Ω in the opposite sense. The angle between $\mathbf{\Omega}$ and the spin is defined as ζ. The resulting motion of the spin $\mathbf{s}$ in space and time can be rather complex. In Figures C.1 to C.3 the projection of the classical spin $\widehat{\mathbf{s}}(t)$ onto the $(\mathbf{x}_0,\mathbf{y}_0)$-plane of the lab system, i.e. $[\sigma_x(t),\sigma_y(t)]$, is shown. (Here we consider $\vec{\sigma}(t) = (2/\hbar)\mathbf{s}(t)$ as a classical Pauli spin).

We introduce in the classical precession the "classical Pauli spin $\vec{\sigma}(t)$" because we showed in the discussion that there is an interpretation of the quantum precession in which the expectation value of the Pauli matrix vector

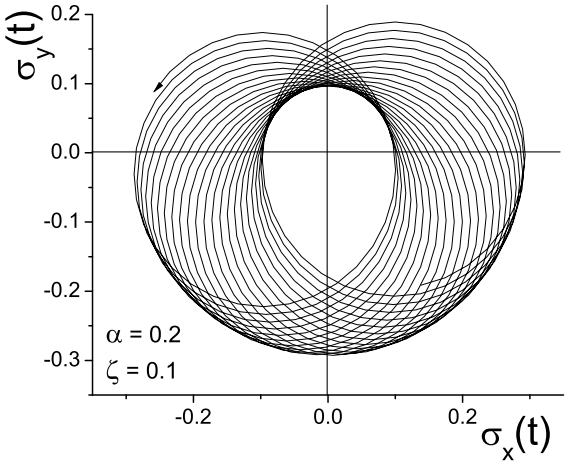

Fig. C.1. The projection of the spin direction in the classical calculation for $\alpha = 0.2$ and $\zeta = 0.1$. The effective precession is counter clockwise.

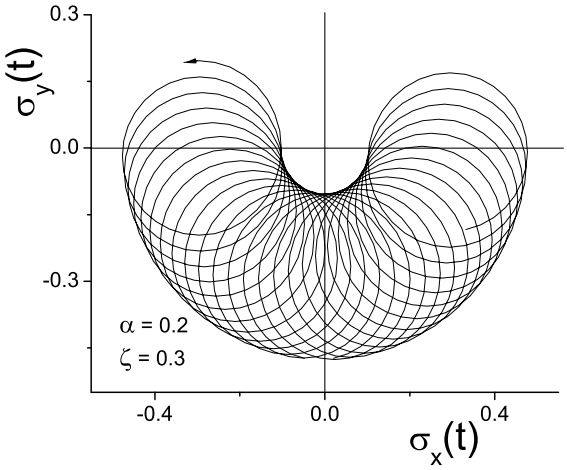

Fig. C.2. The projection of the spin direction in the classical calculation for $\alpha = 0.2$ and $\zeta = 0.3$. The effective precession is clockwise and the effective precession frequency is $\omega_{pcn} = \Omega - \omega_e$.

$\langle\vec{\sigma}\rangle = (\langle\sigma_x\rangle, \langle\sigma_y\rangle, \langle\sigma_z\rangle)$ is identical to the classical (unit vector of the) spin $\widehat{\mathbf{s}}$ and precesses exactly like the latter.

In Figure C.1 the projection of $[\sigma_x(t), \sigma_y(t)]$ is plotted as a function of time for $\alpha = 0.2$ and $\zeta = 0.1$. The dominant part of the motion is the counter clockwise (ccw) rotation of $\mathbf{\Omega}$ with the frequency ω_e about the z-axis (the amplitude is given by $\sin\alpha$). On top of this cycle is the clockwise (cw) precession of $\mathbf{s}$ with the frequency Ω with the angle ζ between $\mathbf{\Omega}$ and $\mathbf{s}$. The direction of motion is shown by the arrow on the left side. Since in Figure C.1 $\zeta < \alpha$ this causes only a deformation of the circle, and each cycle circles the z-axis.

If one defines the effective precession frequency as the frequency with which the symmetry axis is (quasi)-circled then this precession frequency would be essentially given by ω_e.

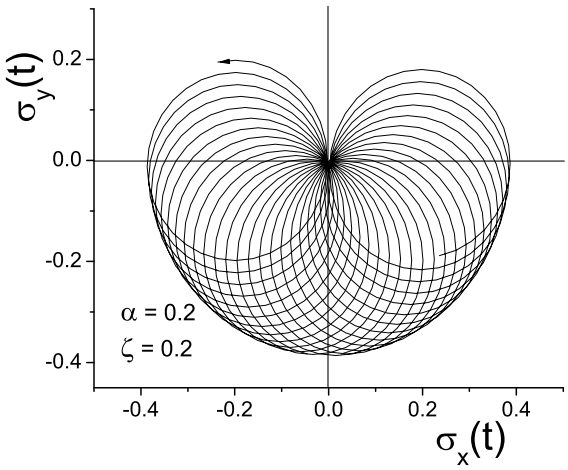

Fig. C.3. The projection of the spin direction in the classical calculation for $\alpha = 0.2$ and $\zeta = 0.2$.

In Figure C.2 the parameters are $\alpha = 0.2$ and $\zeta = 0.3$. Now the unit vector of the spin moves in small circles ccw and the center of the circles moves cw about the z-axis. The motion starts on the right side. The direction of motion is shown by the arrow on the left side. A single circle contributes a rather small part to a circle about the center. The effective frequency of the precession about the z-axis is $\omega_{pcn} = \Omega - \omega_e$. For $\alpha = 0.2$ the value of ω_{pcn} is $0.02\omega_e$.

In Figure C.3 the classical motion of $\widehat{\mathbf{s}}(t)$ is shown for $\alpha = \zeta = 0.2$. Here the individual circles touch the z-axis. The case $\alpha = \zeta$ separates two different regions where a discontinuous jump occurs in the frequency with which the z-axis is cycled by the spin motion.

References

1. S. Manginin, D. Ravelosona, J.A. Katine, M.J. Carey, B.D. Terris, E.E. Fullerton, Nat. Mater. **5**, 210 (2006)
2. A. Neumann, D. Altwein, C. Thoennissen, R. Wieser, A. Berger, A. Meyer, E. Vedmedenko, H.P. Oepen, New J. Phys. **16**, 083012 (2014)
3. F. Haering, U. Wiedwald, S. Nothelfer, B. Koslowski, P. Ziemann, L. Lechner, A. Wallucks, K. Lebecki, U. Nowak, E. Goering, G. Schutz, Nanotechnology **24**, 465709 (2013)
4. A. Parge, T. Niermann, M. Seibt, M. Münzenberg, J. Appl. Phys. **101**, 104302 (2007)
5. S. Khizroev, M.H. Kryder, D. Litvinov, D.A. Thompson, Appl. Phys. Lett. **81**, 2256 (2002)
6. D.P. Weber, D. Rüffer, A. Buchter, F. Xue, E. Russo-Averchi, R. Huber, P. Berberich, J. Arbiol, A.F. Fontcuberta-Morral, D. Grundler, M. Poggio, Nano Lett. **12**, 6139 (2012)
7. J. Lee, D. Suess, T. Schrefl, K.H. Oh, J. Fidler, J. Magn. Magn. Mater. **310**, 2445 (2007)

8. K. Niemirowicz, K.H. Markiewicz, A.Z. Wilczewska, H. Car, Adv. Med. Science **57**, 196 (2012)
9. S.J. Son, J. Reichel, B. He, M. Schuchman, S.B. Lee, J. Am. Chem. Soc. **127**, 7316 (2005)
10. K.Ž. Rozmana, D. Peckoa, S. Sturma, U. Maverb, P. Nadrahb, M. Beleb, S. Kobea, Mater. Chem. Phys. **133**, 218 (2012)
11. H. Hillebrenner, F. Buyukserin, J.D. Stewart, C.R. Martin, Nanomedicine **1**, 39 (2006)
12. J. Xie, L. Chen, V.K. Varadan, S. Chetan, M. Srivatsan, J. Nanotechnol. Eng. Med. **2**, 031009 (2012)
13. P. Landeros, O.J. Suarez, A. Cuchillo, P. Vargas, Phys. Rev. B **79**, 024404 (2009)
14. D. Li, R.S. Thompson, G. Bergmann, J.G. Lu, Adv. Mater. **20**, 4575 (2008)
15. K. Nielsch, F.J. Castaño, C.A. Ross, R. Krishnan, J. Appl. Phys. **98**, 034318 (2005)
16. K.Z. Rozman, D. Pecko, L. Suhodolcan, P.J. McGuiness, S. Kobe, J. Alloys Compd. **509**, 551 (2011)
17. N.A. Usov, O.N. Serebryakova, J. Appl. Phys. **116**, 133902 (2014)
18. G. Bergmann, R.S. Thompson, J.G. Lu, Phys. Lett. A **379**, 2083 (2015)
19. L.H. Thomas, Nature **117**, 514 (1926)
20. J.R. Taylor, in *Classical Mechanics* (University Science Books, 2005), p. 339